J Porous Mater (2017) 24:1661–1665
DOI 10.1007/s10934-017-0406-1

# Facile synthesis of Ag/KIT-6 catalyst via a simple one pot method and application in the CO oxidation

**Yiqiong Yang[1] · Fulin Hou[1] · Hongxin Li[1] · Ning Liu[1] · Yin Wang[1] · Xiaodong Zhang[1]**

Published online: 4 April 2017


**Abstract** Ag/KIT-6 catalyst was successfully synthesized via a simple one pot method for the first time. The structural properties of Ag/KIT-6 catalyst were systematically investigated by X-ray powder diffraction, transmission electron microscope, $N_2$ adsorption–desorption isotherms, and inductively coupled plasma atomic emission spectroscopy. The results showed the synthesized materials exhibited a 3D cubic *la3d* pore structure, and highly uniformly Ag nanoparticles were dispersed on the KIT-6 support. The formation mechanism of Ag/KIT-6 catalyst was also examined. It was found that the obtained Ag/KIT-6 catalyst exhibited better catalytic activity toward CO oxidation.

**Keywords** Ag/KIT-6 · One pot · Oxidation · Porous materials

## 1 Introduction

Nanosized Ag particles have received considerable interest in recent years due to unique physical and chemical properties, such as optical and electrical, which makes it desirable for use in catalysis and optical devices [1, 2]. Mesoporous materials are a promising candidate for the support of nanostructured metals due to their narrow pore size distribution, high specific surface area and large pore volume [3, 4]. The one pot method is the most simple among the investigated methods to fabricate metal particles. Up to date, a series of mesoporous silica with uniform pores, such as SBA-15, and HMS, have received attention as support for the preparation of supported Ag catalysts [5–11]. Zhu et al. have reported that Ag was incorporated in the framework of SBA-15 by in-situ synthesis method in strongly acidic media [5]. Tian et al. have synthesized Ag/SBA-15 nanocomposites by in-situ reduction method [6]. Our previous results showed highly ordered Ag/SBA-15 nanocomposites were synthesized by "pH-adjusting" method [7–9]. In addition, a novel and simple one pot synthesis approach has been employed to synthesize Ag/HMS catalyst [10, 11].

Recently, special attention has been paid to KIT-6, which consists of three dimensional (3D) cubic *Ia3d* mesostructure with two interpenetrating continuous networks of chiral channels [12]. This unique 3-D channel network could provide a highly opened porous host with easy and direct access for guest species, thereby facilitating inclusion or diffusion throughout the pore channels without pore blockage. However, due to $Cl^-$ or *n*-butanol of synthesis solution [12–14], it is difficult to incorporate Ag precursor into the channels of KIT-6 by using one-pot method. In order to solve the above problems that $Ag^+$ reacts with $Cl^-$ or *n*-butanol, the synthesis method without *n*-butanol was selected. Moreover, HCl and NaCl were replaced to $HNO_3$ and $NaNO_3$, respectively. Herein, we report a simple one pot method that is more facile and effective to synthesize highly ordered Ag/KIT-6 catalyst, which is highly active for CO oxidation.

✉ Xiaodong Zhang
fatzhxd@126.com

[1] School of Environment and Architecture, University of Shanghai for Science and Technology, Shanghai 200093, China

## 2 Experimental

### 2.1 Sample preparation

In a typical synthesis, 2.84 g of triblock copolymer P123 ($EO_{20}PO_{70}EO_{20}$) and 10.471 g sodium nitrate were dissolved in 160 ml of nitric acid solution (0.5 M). The mixture was stirred at 40 °C until a homogenous solution formed under acidic conditions. 0.2015 g of silver nitrate was added to the solution and stirred for 3 h at the same temperature in the dark. Then, 4.75 ml of tetraethoxysilane (TEOS) and 1.12 ml triethoxyvinylsilane (TEVS) were added to the solution and stirred for 20 h at 40 °C in the dark. The final molar ratio was TEOS: TEVS: $NaNO_3$: P123: $AgNO_3$: $HNO_3$: $H_2O$ = 1 : 0.25 : 5.78 : 0.023 : 0.055 : 4.34 : 406.5. The mixture was aged at 100 °C for 48 h in a polypropylene bottle without stirring in the dark. After cooling to room temperature, the resulting solid was filtered, washed with deionized water, and then dried under ambient conditions. Finally, the solid was calcined at about 550 °C for 5 h in air to obtain Ag/KIT-6 catalyst. The preparation routes of pure-silica KIT-6, which was employed as reference, were the same as that of Ag/KIT-6 catalyst except that no silver nitrate was added into the nitric acid solution.

### 2.2 Characterization

Routine X-ray powder diffraction (XRD) experiments were carried out on a Bruker D8 Advance X-ray diffractometer by a monochromatic detector equipped with Ni-filtered Cu Kα radiation (λ = 1.541874 Å). Copper Kα radiation was used, with a power setting of 40 kV and 40 mA, and a scan rate of 5° $min^{-1}$ (and a scan rate of 2° $min^{-1}$ for small-angle X-ray scanning). High-resolution TEM experiments were obtained with a FEI Tecnai G2 F20 microscope. For the TEM analysis, a sample was dispersed in absolute alcohol by an ultrasonic bath and deposited on a Formvar coated 200 mesh Cu grids. The ICP-AES was used to determine the content of silver in the synthesized samples, which was performed on an OPTIMA 2000. The $N_2$ adsorption/desorption isotherms at about −196 °C were measured using a Quantachrome autosorb-iQ-2MP gas sorption analyzer. The specific surface area was calculated by using the BET (Brunauer–Emmett–Teller) model. The pore size distributions were determined by the BJH (Barrett–Joyner–Halenda) method using the desorption branch of the isotherms.

### 2.3 Catalytic activity measurements

CO oxidation activity measurements were carried out in a fixed-bed flow reactor (6 mm outside diameter) at atmospheric pressure. 0.2 g of catalyst with 20–40 mesh was used. The reactants were fed with a volume ratio of He/CO/$O_2$ = 79/1/20 at a total flow rate of 30 ml/min, which was controlled by an independent thermal mass flow controller. On-line gas chromatograph (GC 2060, China Shanghai Ruimin Co.) with a TCD detector was employed to measure the reactor inlet and outlet effluent gas streams. 5 A molecular sieves column (3 m × 3 mm) was used to separate oxygen, carbon monoxide. Before the reaction, the catalyst was pretreated with $O_2$ at 600 °C for 2 h, followed by $H_2$ at 200 °C for 1 h at a flow rate of 30 ml/min.

### 2.4 Results and discussion

The low angle XRD patterns of KIT-6 and Ag/KIT-6 catalyst are shown in Fig. 1a. The KIT-6 exhibits a sharp intense peak at 2θ of 1.17° and another peak at 2θ of 1.35°, which correspond to the (211) and (220) planes, respectively. The peak is the characteristic of body-centered cubic *la3d* group of 3D mesoporous silica [12, 13]. After the addition of Ag, the intensity of the peaks is reduced; simultaneously, the diffraction peak is shifted to higher 2θ values. This result is attributed to the channels of KIT-6 being partly blocked by Ag, which is consistent with the reports in literatures [2, 7, 15]. Figure 1b shows the wide-angle XRD pattern of Ag/KIT-6 catalyst. The sample exhibits four intense diffraction peaks, corresponding to the (111), (200), (220), and (311)

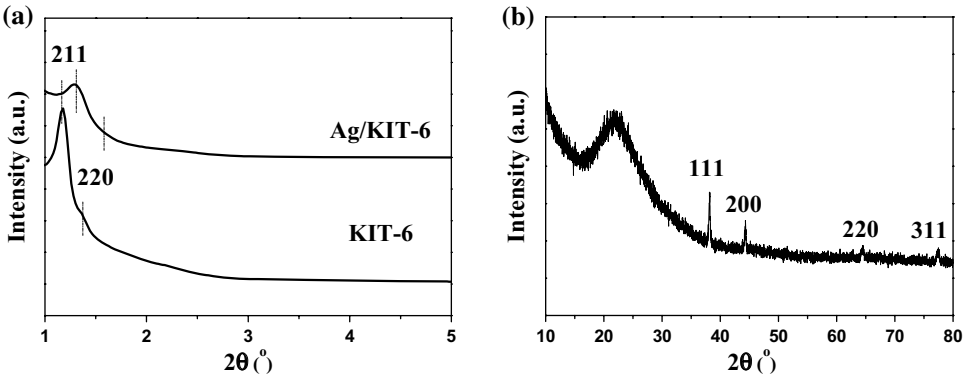


**Fig. 1** **a** The low angle XRD patterns of KIT-6 and Ag/KIT-6 catalyst; **b** the wide angle XRD pattern of Ag/KIT-6 catalyst calcined at 600 °C

lattice planes of the cubic structure of Ag, respectively. The broad peak at about 2θ = 22° is ascribed to the amorphous silica. In order to gain a deep insight into the pore morphology and silver nanoparticles distribution, these materials were further characterized by TEM and HRTEM micrographs (Fig. 2). Figure 2a shows an overview of the Ag/KIT-6 catalysts. The well-ordered characteristic structures offer further evidence that the sample is 3D ordered pore structure (Fig. 2b). Moreover, many highly dispersed Ag nanoparticles are observed in the surface and channels of KIT-6. The fringes in Fig. 2c give a d-spacing of 0.23 nm, corresponding to the (111) atomic planes of the cubic silver lattices. As seen in Fig. 2d, Ag particles with uniform size of around 4–7 nm and well dispersed on the KIT-6 support.

Figure 3 shows the $N_2$ adsorption–desorption isotherms of KIT-6 and Ag/KIT-6 catalyst. The two samples both show typical IV adsorption–desorption isotherms with H1-type hysteresis, indicating the presence of framework mesoporosity [12, 13]. Compared with KIT-6, the hysteresis loop for Ag/KIT-6 catalyst moves to a relatively lower pressure, simultaneously, the specific surface area, pore size and total pore volume decrease from 527 $m^2g^{-1}$, 6.6 nm and 0.94 $cm^3g^{-1}$ (KIT-6) to 411 $m^2g^{-1}$, 4.9 nm and 0.63 $cm^3g^{-1}$ (Ag/KIT-6), respectively. The previous

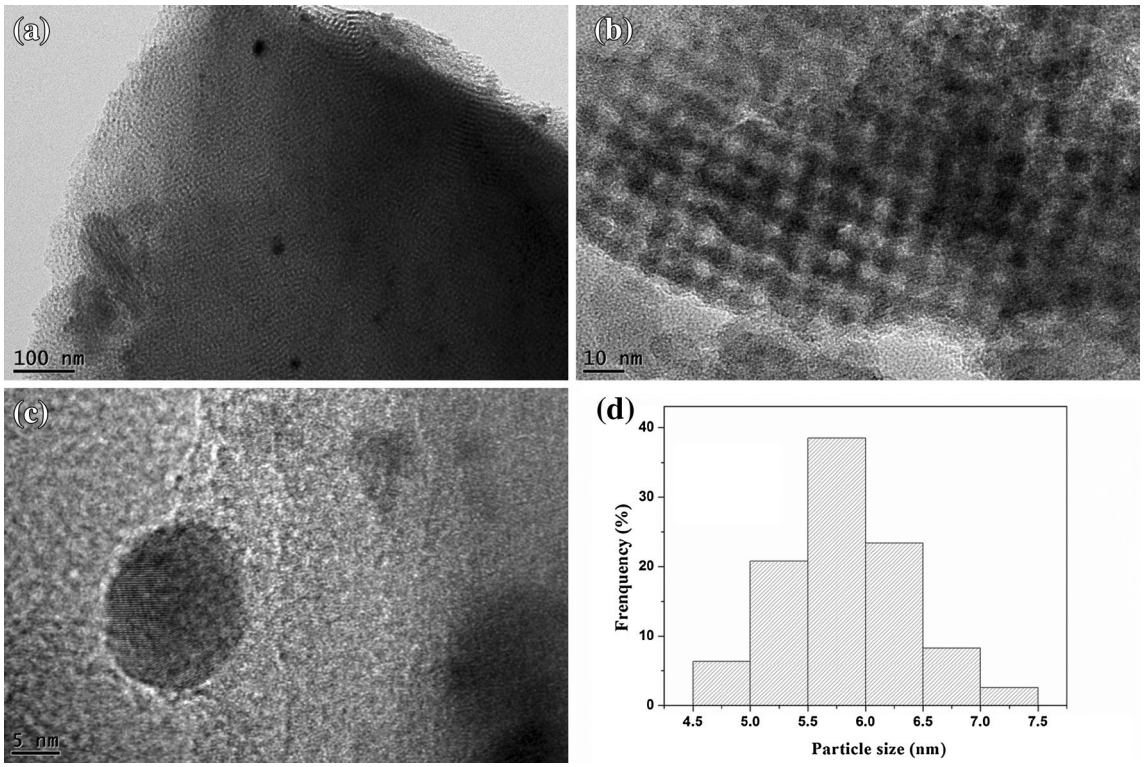


**Fig. 2** TEM, HRTEM images and the corresponding particle size distribution of Ag/KIT-six catalyst calcined at 600 °C

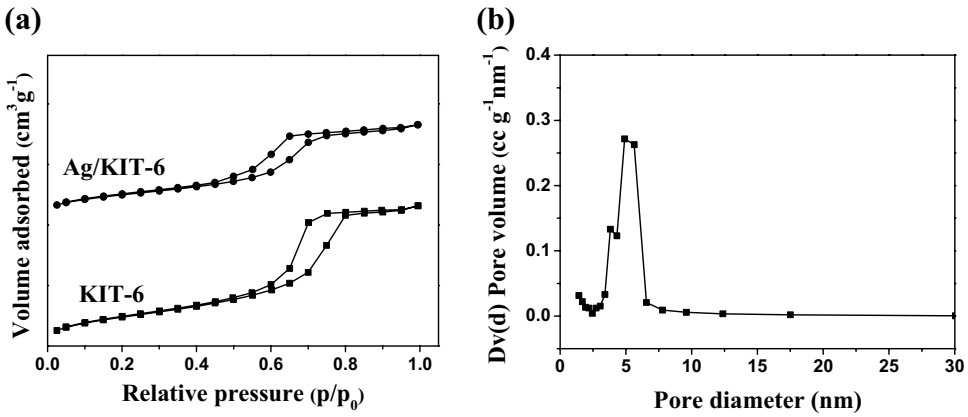


**Fig. 3** **a** The $N_2$ adsorption–desorption isotherms of KIT-6 and Ag/KIT-6 catalyst; **b** the pore size distributions of Ag/KIT-6 catalyst calcined at 600 °C

studies showed the progressive incorporation of Ag particles inside the channels of SBA-15 resulted in the decrease in the pore size [7, 16]. Thus, the decrease in the pore size could be attributed to the progressive blockage due to the incorporated Ag particles inside the channels of KIT-6, in good accordance with the above low-angle XRD and TEM results.

In order to further study the formation process of Ag particles, the XRD of Ag/KIT-6 prepared under different conditions are characterized (Fig. 4). Obvious diffraction peaks of Ag particles appear over uncalcined Ag/KIT-6 (Fig. 4a), which revealed silver particles have formed during the preparation process. Interestingly, no diffraction peaks of silver or silver compounds are found over uncalcined Ag/KIT-6 prepared without the crystallization procedure (Fig. 4c). Therefore, it is believed that Ag particles formed during the crystallization procedure without reductant and/or calcination. Our previous studies found that the silver ions of Ag/SBA-15 would be automatically reduced to silver atoms during the dehydration of EO units [9]. Thus it is explained the reason of Ag/KIT-6 with high silver content (3.78 wt%).

Here, the formation process of Ag/KIT-6 catalyst involves the following four stages: (1) when surfactant P123 was dissolved in $HNO_3$ solution, the micelles are formed; (2) $AgNO_3$ are adsorbed on the EO units' surfaces to form the metal-block copolymer hybrid with the micelles through weak coordination bonding after adding metal precursor [17]; (3) when a certain proportion of TEVS/TEOS is added, TEVS and existing salts in the stage 1 will be preferentially adsorbed close to the hydrophobic PPO portion of the micelles, which decreased the preferential interfacial curvature of the inorganic–organic assembly, finally favoring the formation of the *Ia3d* phase over the 2D hexagonal phase [13]. (4) crystallization procedure completes the condensation of the silica species into the *Ia3d* phase mesostructures materials, and silver ions are reduced to metal silver particles.

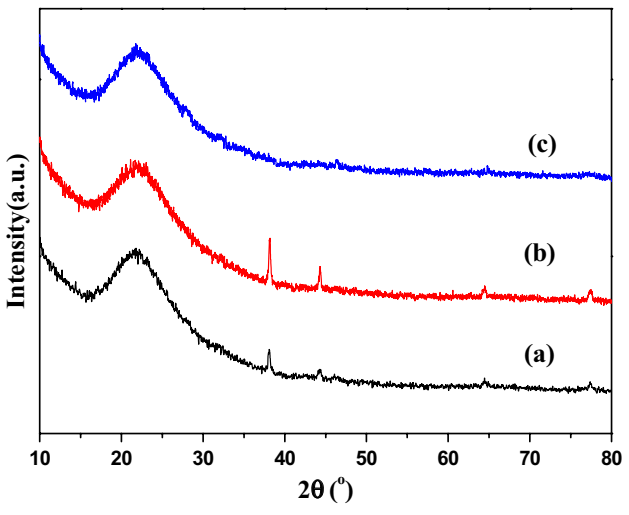


**Fig. 4** The wide angle XRD pattern of Ag/KIT-6 catalyst prepared without calcination (*a*), Ag/KIT-6 catalyst (*b*) and Ag/KIT-6 catalyst prepared without the crystallization procedure and calcination (*c*)

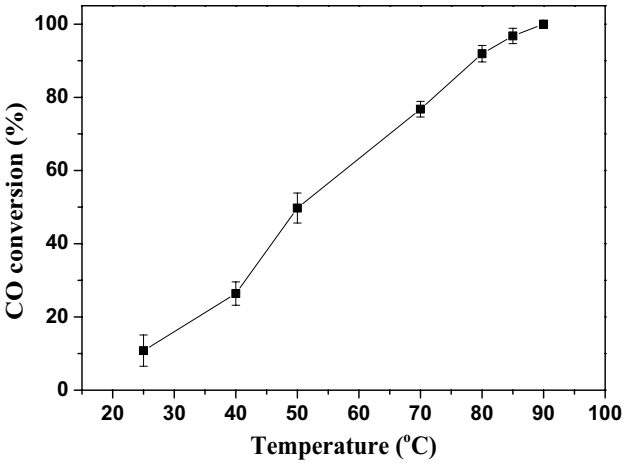


**Fig. 5** CO conversion over Ag/KIT-6 catalyst after $H_2$ treatment at 200 °C

The CO catalytic performance of the obtained Ag/KIT-6 catalyst toward CO oxidation is presented in Fig. 5. The $H_2$ treatment at 200 °C was done before the activity tests. The $T_{50}$ and $T_{100}$ values (corresponding to CO conversion = 50 and 100%) for Ag/KIT-6 catalyst are about 50 and 90 °C, respectively. Compared with recently reported Ag catalysts [18], such as Ag/KCC-1, Ag/SBA-15, Ag/MCM-41, Ag/$SiO_2$, our Ag/KIT-6 catalyst displays higher catalytic activity. In addition, according to our acquired turnover frequencies (TOFs = 1.24) for CO at 25 °C, our Ag/KIT-6 catalyst displays better behavior toward CO oxidation than those of reported Ag/SBA-15 catalysts prepared by one pot method [6, 8]. In addition, a better stability in initial stage (48 h)

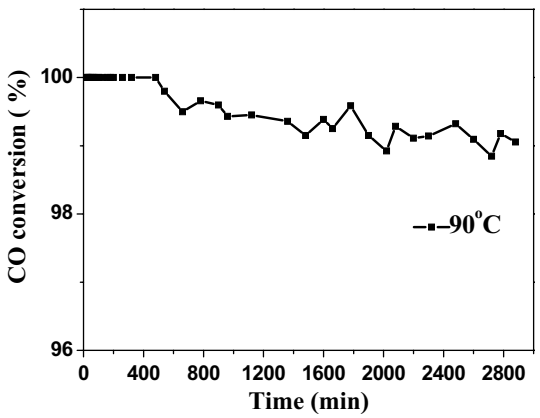


**Fig. 6** Stability study of Ag/KIT-6 catalyst after $H_2$ treatment at 200 °C

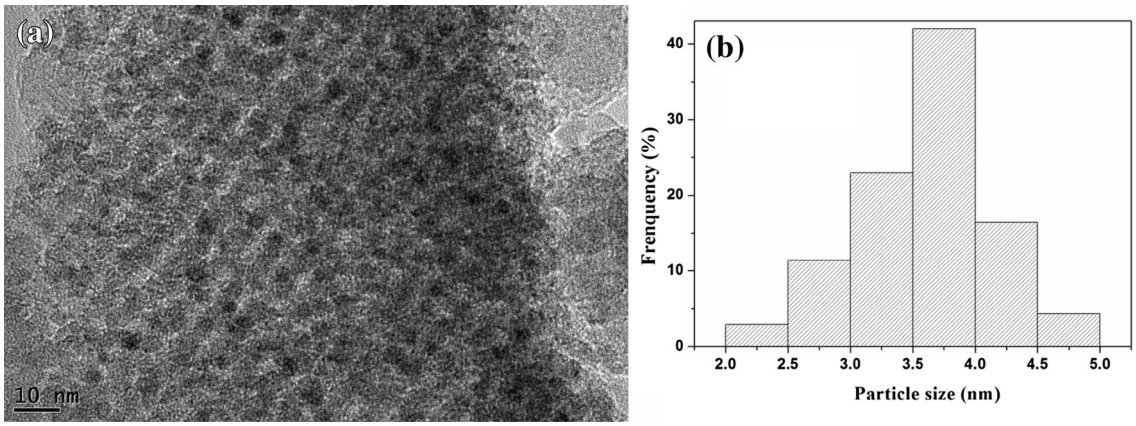


**Fig. 7** TEM and the corresponding particle size distribution of Ag/KIT-6 catalyst after $H_2$ treatment at 200 °C

for CO oxidation at 90 °C is also obtained (Fig. 6). Tian et al. have reported the 100% CO conversion of 5.28 wt% Ag/SBA-15 catalyst at 230 °C [6]. Our previous results have showed the TOFs of 7.8 wt% Ag/SBA-15 catalyst was 0.83 [8]. In addition, Soni et al. have found that KIT-6 supported catalysts showed superior activities in comparison with γ-$Al_2O_3$ and SBA-15 supported catalysts, which was attributable to 3-D mesopore connectivity resulting in better catalyst dispersion, higher reducibility of Mo, and faster diffusion of reactant and products in the KIT-6 supported catalysts [19]. TEM results (Fig. 7) further indicate that Ag particle size of $H_2$- treated catalysts become much smaller as compared to untreated catalyst (Fig. 2). It is found that the Ag particles are more uniformly dispersed on the KIT-6 support, and small Ag particles with narrow size distribution (2–5 nm) are observed. Thus, in the paper, Ag/KIT-6 catalyst prepared by one pot method shows a better performance, which may be due to 3D channel of KIT-6 resulting in faster diffusion of reactant and products and better Ag dispersion.

## 3 Conclusions

In summary, high-quality Ag/KIT-6 catalyst can be directly synthesized by the one pot synthesis method for the first time. The Ag/KIT-6 catalyst still preserves well-defined mesostructures, and highly uniformly Ag nanoparticles were dispersed on the KIT-6 support. The obtained Ag/KIT-6 catalyst exhibited better catalytic activity toward CO oxidation.

**Acknowledgements** This work was sponsored financially by the National Natural Science Foundation of China (No.21507086, 51508327) and Shanghai Sailing Program (14YF1409900, 16YF1408100).

## References

1. G. Schmid, M. Baumle, M. Geerkens, I. Heim, C. Osemann, T. Sawitowski, Chem. Soc. Rev. **28**, 179 (1999)
2. P.V. Adhyapak, P. Karandikar, K. Vijayamohanan, A.A. Athawale, A.J. Chandwadkar, Mater. Lett. **58**, 1168 (2004)
3. J.S. Kresge, M.E. Leonowicz, W.J. Roth, Nature **359**, 710 (1992)
4. D. Zhao, J. Feng, Q. Huo, N. Melosh, G.H. Fredrickson, B.F. Chmelka, G.D. Stucky, Science **279**, 548 (1998)
5. W.P. Zhu, Y.C. Han, L.J. An, Microporous Mesoporous Mater. **80**, 221 (2005)
6. D. Tian, G.P. Yong, Y. Dai, X.Y. Yan, S.M. Liu, Catal. Lett. **130**, 211 (2009)
7. X.D. Zhang, Z.P. Qu, X.Y. Li, Q.D. Zhao, X. Zhang, X. Quan, Mater. Lett. **65**, 1892 (2011)
8. X.D. Zhang, Z.P. Qu, X.Y. Li, Q.D. Zhao, X. Zhang, X. Quan, Catal. Commun. **16**, 11 (2011)
9. Z.P. Qu, X.D. Zhang, Y. Lv, X. Quan, Q. Fu, J. Nanosci. Nanotech. **13**, 4573 (2013)
10. X.D. Zhang, Z.P. Qu, J.X. Jia, Y. Wang, Power. Technol. **230**, 212 (2012)
11. Z.P. Qu, X.D. Zhang, F.L. Yu, J.X. Jia, Microporous Mesoporous Mater. **188**, 1 (2014)
12. F. Kleitz, C.S. Hei, R. Ryoo, Chem. Commun. **17**, 2136 (2003)
13. Y.Q. Wang, C.M. Yang, B. Zibrowius, B. Spliethoff, M. Lindén, F. Schüth, Chem. Mater. **15**, 5029 (2003)
14. Y.Y. Li, Y.H. Zhang, L.P. Jiang, P.K. Chu, Y. Dong, P. Wang, RSC Adv. **6**, 6932 (2016)
15. M.H. Lim, A. Stein, Chem. Mater. **11**, 3285 (1999)
16. A.Y. Yin, C. Wen, W.L. Dai, K.N. Fan, Appl. Catal. B **108–109**, 90 (2011)
17. H.F. Yang, Q.H. Shu, B.Z. Tian, Q.Y. Lu, F. Gao, S.H. Xie, J. Fan, C.Z. Yu, B. Tu, D.Y. Zhao, J. Am. Chem. Soc. **125**, 4724 (2003)
18. J. Xu, J.Y. Zhang, H.G. Peng, X.L. Xu, W.M. Liu, Z. Wang, N. Zhang, X. Wang, Microporous Mesoporous Mater. **242**, 90 (2017)
19. K. Soni, B.S. Rana, A.K. Sinha, A. Bhaumik, M. Nandi, M. Kumar, G.M. Dhar, Appl. Catal. B **90**, 55 (2009)